Relativistic transformations of quasi-monochromatic paraxial optical beams

Murat Yessenov and Ayman F. Abouraddy
CREOL, The College of Optics & Photonics, University of Central Florida, Orlando, Florida 32816, USA

(Received 8 August 2022; accepted 11 April 2023; published 27 April 2023)

A monochromatic plane wave recorded by an observer moving with respect to the source undergoes a Doppler shift and spatial aberration. We investigate here the transformation undergone by a generic, paraxial, spectrally coherent quasimonochromatic optical *beam* (of finite transverse width) when recorded by a moving detector. Because of the space-time coupling intrinsic to the Lorentz transformation, the monochromatic beam is converted into a propagation-invariant pulsed beam traveling at a group velocity equal to that of the relative motion and which belongs to the recently studied class of "space-time wave packets." We show that the predicted transformation from a quasimonochromatic beam to a pulsed wave packet can be observed even at terrestrial speeds.

DOI: 10.1103/PhysRevA.107.042221

An observer moving with respect to an optical source emitting a monochromatic plane wave (MPW) records a Doppler-shifted MPW [1–4]. What are the changes observed by a detector moving with respect to a source emitting instead a generic monochromatic optical *beam* (i.e., a transversely localized field)? Previously tackled questions regarding relativistic transformations of optical fields have sometimes revealed surprising answers. For example, Terrell [5] and Penrose [6] showed that the length of an object in an image captured by an instantaneous shutter does *not* depend on the observer's velocity, thus disabusing the physics community of the notion of a "visible" Lorentz contraction [7]. Recently, it was shown that angular-momentum-carrying optical fields exhibit exotic effects in a frame moving orthogonally to the optical axis, including an optical analog of the relativistic spin Hall effect [8,9], transverse orbital angular momentum and spatiotemporal vortices [10,11], and relativistic spin-orbit interactions [12].

We analyze here the transformation of monochromatic and quasimonochromatic paraxial generic beams when recorded by an observer moving with respect to the source along the beam axis. Because the Lorentz transformation introduces space-time coupling [13,14] into the optical field, it converts a strictly *monochromatic* beam in one frame into a finite-bandwidth *pulsed* beam in any other frame. Previous studies [15,16] focused on Lorentz transformations yielding so-called focus-wave modes (FWMs) [17] and X-waves [18], which are propagation-invariant pulsed beams [19,20]. However, FWMs and X-waves require exorbitant bandwidths for their characteristics to deviate observably from a conventional pulsed beam [21]. The Lorentz transformation of light emitted by an optical dipole (which is *not* paraxial) [16,22] corresponds to the so-called Mackinnon wave packet [23], which is yet to be realized.

Recently, a new class of propagation-invariant pulsed fields denoted "space-time wave packets" (STWPs) has been pursued [24–29], which has proven more accessible experimentally. In contrast to FWMs and X-waves, STWPs can be synthesized with narrow bandwidths within the paraxial regime and have been shown to display a host of unique characteristics including tunable group velocity [30], self-healing [31], and anomalous refraction [32] (see [21] for a review of this emerging area). Here we show that STWPs result from the Lorentz transformations of generic, paraxial, monochromatic, or spectrally coherent quasimonochromatic optical beams. In other words, an observer in relative motion with respect to such beams will record an STWP of the kind only recently synthesized in the laboratory via spatiotemporal spectral modulation [21]. Moreover, the group velocity of the induced wave packet is the relative velocity between the source and detector [33,34].

We first provide a physically intuitive picture that underpins the conversion of generic, strictly monochromatic paraxial beams (regardless of the details of the spatial beam structure) into ideal propagation-invariant STWPs in terms of their representation on the surface of the spectral light-cone. In particular, we identify the impact of the transverse *spatial* beam width on the *temporal* pulse-width of the induced wave packet via the angular-dependent Doppler shift. Next, we extend our analysis to more realistic quasimonochromatic paraxial beams and show that the departure from monochromaticity imposes a maximum propagation distance on the generated STWP before the onset of diffractive spreading, which in turn determines a minimum relative observer velocity for these effects to be detectable. Finally, we suggest a road map for experiments based on the relative motion of ultranarrow-linewidth optical sources and detectors and examine the potential for observing such effects at terrestrial speeds with currently available lasers.

To set the stage for analyzing the Lorentz transformation of optical beams, we first examine the case of MPWs in one transverse dimension x (without loss of generality); see Fig. 1. An MPW at frequency ω emitted by a source $\mathcal{S}$ at rest in the inertial frame $\mathcal{O}(x,z,t)$ is Doppler-shifted to $\omega'=\sqrt{\frac{1-\beta}{1+\beta}}\omega$ in the frame $\mathcal{O}'(x',z',t')$ moving at a velocity $v=\beta c$ along the common z axis [Fig. 1(a)]. An MPW traveling in $\mathcal{O}$ at an angle φ with the z axis is transformed in $\mathcal{O}'$ to a frequency

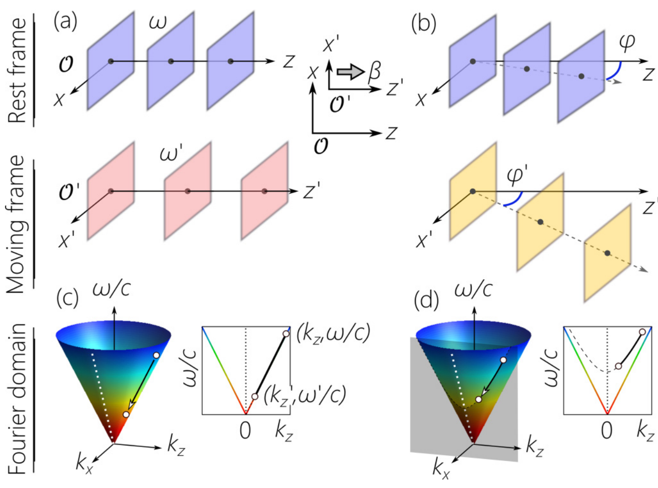

FIG. 1. A MPW emitted in the rest frame $\mathcal{O}$ is Doppler-shifted in the frame $\mathcal{O}'$ moving along the $+z$ axis. (b) An off-axis MPW in $\mathcal{O}$ is Doppler-shifted and undergoes an angular rotation in $\mathcal{O}'$. (c) The on-axis MPW is Doppler-shifted along the light line $k_z=\omega/c$ ($k_x=0$) in the Fourier domain, whereas (d) an off-axis MPW is shifted along a fixed-k_x hyperbola on the light-cone surface.

$\omega'=\gamma(1-\beta\cos\varphi)\omega$ traveling at an angle $\varphi'=\cos^{-1}[\frac{\cos\varphi-\beta}{1-\beta\cos\varphi}]$ (the Doppler spatial aberration [3]), where $\gamma=1/\sqrt{1-\beta^2}$ [Fig. 1(b)].

These changes can be visualized on the surface of the spectral light-cone [29,35]. The wave vector $\vec{k}=(k_x,k_z)$ for an MPW in $\mathcal{O}$ is represented by a point on the surface $k_x^2+k_z^2=(\frac{\omega}{c})^2$, where $k_x=\frac{\omega}{c}\sin\varphi$ and $k_z=\frac{\omega}{c}\cos\varphi$. The Lorentz-transformed wave-vector components are $k_x'=k_x$, $k_z'=\gamma(k_z-\beta\omega/c)$, and $\omega'=\gamma(\omega-c\beta k_z)$. Because $k_x'^2+k_z'^2=(\frac{\omega'}{c})^2$, the structure of the light-cone itself is Lorentz-invariant so that the points corresponding to MPWs in $\mathcal{O}$ and $\mathcal{O}'$ can be represented on the same surface. The MPW in Fig. 1(a) corresponds to a point on the light-line $k_x=0$, along which its Doppler-shifted counterpart in $\mathcal{O}'$ is displaced [Fig. 1(c)]. In contrast, the point representing the off-axis MPW in $\mathcal{O}$ [Fig. 1(b)] is displaced in $\mathcal{O}'$ along a constant-k_x hyperbola [Fig. 1(d)].

Now consider a generic monochromatic *beam* of transverse width Δx emitted by the source $\mathcal{S}$ in $\mathcal{O}$ [Fig. 2(a)], which is a superposition of plane waves (spatial bandwidth $\Delta k_x\sim\frac{1}{\Delta x}$) all at the same frequency ω_o but traveling at different angles φ with the z axis [36,37]. The spectral support for the beam is a circle $k_x^2+k_z^2=k_o^2$ at the intersection of the light-cone with a horizontal isofrequency plane $\omega=\omega_o$ [Fig. 2(b)]; here $k_o=\omega_o/c$. We write the field as $E(x,z;t)=e^{i(k_oz-\omega_ot)}\psi(x,z)$, where $\psi(x,z)$ is a slowly varying envelope of angular spectrum

$$\psi(x,z)=\int dk_x\widetilde{\psi}(k_x)e^{ik_xx}e^{i(k_z-k_o)z};\tag{1}$$

here the spatial spectrum $\widetilde{\psi}(k_x)=\int dx\,\psi(x,0)e^{-ik_xx}$ is the Fourier transform of the initial profile $\psi(x,0)$.

Applying the Lorentz transformation between the coordinates (x',z',t') and (x,z,t): $x=x'$, $z=\gamma(z'+\beta ct')$, and $t=\gamma(t'+\beta z'/c)$, the transformed field $E'(x',z';t')=E(x,z;t)$ takes the form [15,33]

$$\begin{aligned}E'(x',z';t')&=E[x',\gamma(z'+\beta ct');\gamma(t'+\beta z'/c)]\\&=e^{i(k_o'z'-\omega_o't')}\psi[x',\gamma(z'+vt')],\end{aligned}\tag{2}$$

where $\omega_o'=\gamma(1-\beta)\omega_o$ is the Doppler-shifted carrier frequency and $k_o'=\omega_o'/c$. It is clear from Eq. (2) that the field in $\mathcal{O}'$ corresponds to a propagation-invariant pulsed beam traveling at a group velocity $\widetilde{v}=-v$. The on-axis pulse-width $\Delta T'$ of this propagation-invariant wave packet is dictated by the Rayleigh range z_R of the monochromatic beam in $\mathcal{O}$: $\Delta T'=z_R/(\gamma v)$.

An intuitive physical picture is based on the field representation in the spectral domain. Because the Doppler shift depends on the relative velocity v and angle φ, the MPWs in $\mathcal{O}$ undergo *different* spectral shifts in $\mathcal{O}'$ [Fig. 2(c)] and

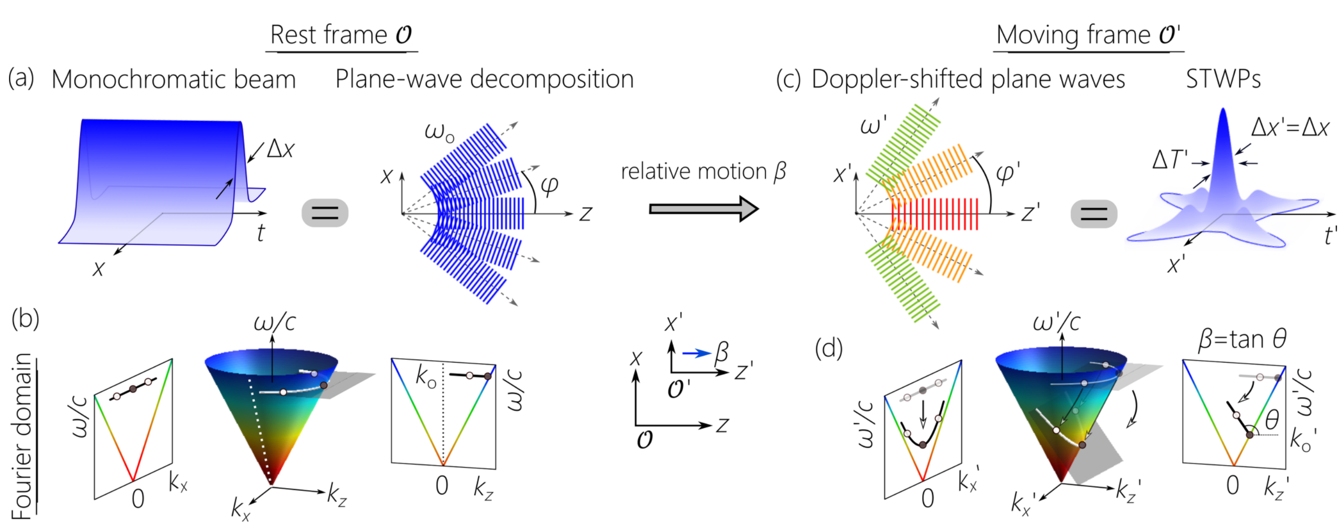

FIG. 2. Lorentz transformation of a monochromatic beam. (a) A monochromatic beam in $\mathcal{O}$ is a superposition of plane waves of the *same* frequency ω_o traveling in *different* directions, and (b) its spectral support on the light-cone is an isofrequency circle. (c) In the moving frame $\mathcal{O}'$, each plane wave undergoes an angle-dependent Doppler shift. (d) The spectral support for the field in (c) is the intersection of the light-cone with a plane that makes an angle θ with the k_z' axis.

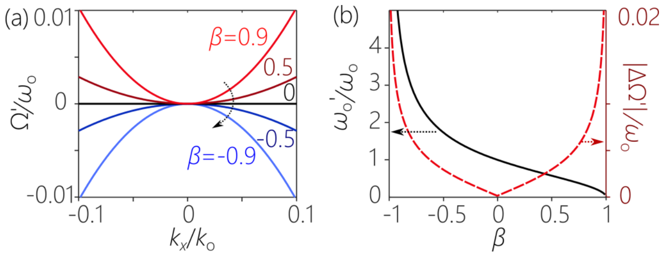

FIG. 3. (a) Spatiotemporal spectrum of paraxial STWPs in $\mathcal{O}'$ for different observer velocities β. (b) Dependence of the STWP central frequency ω_o' (black solid curve, left axis) and bandwidth $|\Delta\Omega'|$ (red dashed curve, right axis) on β, normalized to the frequency ω_o of the monochromatic beam in $\mathcal{O}$ having $\Delta k_x = 0.1k_o$.

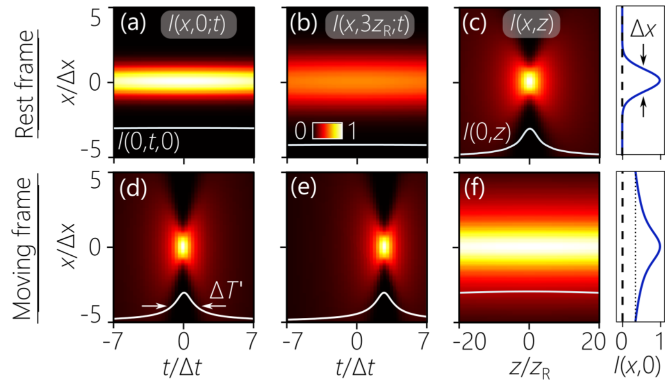

FIG. 4. (a) Spatiotemporal intensity profile $I(x,z;t)$ at the axial plane $z=0$ and (b) at $z=3z_R$ in the rest frame $\mathcal{O}$. (c) The time-averaged intensity $I(x,z)$ in $\mathcal{O}$. (d) Spatiotemporal intensity profile $I(x',z';t')$ at $z'=0$ and (e) at $z'=3z_R$ in $\mathcal{O}'$. (f) The time-averaged intensity $I(x',z')$ in $\mathcal{O}'$.

the associated points along the circle on the light-cone in $\mathcal{O}$ are displaced in $\mathcal{O}'$ differently along constant-k_x hyperbolas [Fig. 2(d)]. Consequently, a finite bandwidth $\Delta\omega'$ is induced in the initially monochromatic beam whose coherence guarantees that the space-time-coupled field in $\mathcal{O}'$ is *pulsed* [Fig. 2(c)]. The spectral support is transformed from a horizontal circle in $\mathcal{O}$ into a tilted ellipse in $\mathcal{O}'$ [34] at the intersection of the light-cone with the plane $k_z'-k_o'=(\omega'-\omega_o')/(c\tan\theta)$, which is parallel to the k_x axis, but makes an angle θ with the k_z' axis, where $\tan\theta=-\beta$ [Fig. 2(d)]. The linear relationship between k_z' and ω' indicates a dispersion-free wave packet traveling rigidly in $\mathcal{O}'$ without diffraction at a group velocity $\widetilde{v}=c\tan\theta=-v$ [30,38]. This dispersion relationship is identical to the dispersion relationship characteristic of STWPs [21,38]. Thus, a generic diffracting monochromatic beam in the rest frame $\mathcal{O}$ is transformed into a propagation-invariant STWP in the moving frame $\mathcal{O}'$. In the paraxial regime $\Delta k_x \ll k_o$, the ellipse in $\mathcal{O}'$ can be approximated by a parabola $\Omega'(k_x')=\frac{ck_x'^2}{2k_o'(1-\cot\theta)}$ [Fig. 3(a)], where $\Omega'=\omega'-\omega_o'$ [38]. The initially monochromatic beam acquires a bandwidth $\Delta\Omega'=\frac{1}{2}\gamma|\beta|\omega_o(\frac{\Delta k_x}{k_o})^2$ via space-time coupling. Although $\Delta\Omega'$ is independent of the sign of β (i.e., it is symmetric with respect to approaching or receding observers), the carrier frequency ω_o' in contrast is highly asymmetric around $\beta=0$ [Fig. 3(b)]. Such a field corresponds to a so-called subluminal "baseband" STWP [21,29], which have been recently synthesized with group velocities in the range $0.07c<\widetilde{v}<c$ [30,39]. It will, of course, be challenging to produce such STWPs via relative motion between a source and detector.

Crucially, these conclusions are independent of the particular beam structure. As a generic example, take a monochromatic Gaussian beam at ω_o in $\mathcal{O}$ with $\widetilde{\psi}(k_x)\propto\exp\{-\frac{k_x^2}{2(\Delta k_x)^2}\}$. The time-resolved intensity $I(x,z;t)=|E(x,z;t)|^2$ at any axial plane z is, of course, independent of time [Figs. 4(a) and 4(b)]. Consequently, a "fast" detector recording $I(x,z;t)$ or a "slow" detector capturing the time-averaged intensity $I(x,z)=\int dt\, I(x,z;t)$ both reveal the *same* spatial Gaussian envelope in $\mathcal{O}$ [Fig. 4(c)].

In $\mathcal{O}'$, the spatiotemporal spectrum is $\widetilde{\psi}(k_x',\omega')=\widetilde{\psi}(k_x')\delta[\Omega'-\Omega'(k_x')]$, leading to an envelope

$$\psi(x',z';t')=\iint dk_x'd\Omega'\;\widetilde{\psi}(k_x',\Omega')e^{i[k_x'x'+(k_z'-k_o')z-\Omega't']},\quad(3)$$

which is propagation invariant $\psi(x',z';t')=\psi(x',0;t'-z'/\widetilde{v})=\psi(x',z'-\widetilde{v}t';0)$, with $\widetilde{v}=c\tan\theta=-v$. That is, the roles of time and the axial coordinate $z'/\widetilde{v}$ are interchanged: the spatial profile along z for a monochromatic beam in $\mathcal{O}$ [Fig. 4(c)] is now observed in time at a fixed axial plane in $\mathcal{O}'$ [Figs. 4(d) and 4(e)]. This phenomenon was predicted in [33] and called "diffraction in time" (which is distinct from "time-diffraction" [40–42]) and verified experimentally in [34]. The invariance of k_x in frames moving along z guarantees that Δx is invariant. The time-averaged intensity $I(x',z')=I_o+I_{ST}(x')$ [43] is now independent of z' and takes the form of a constant pedestal I_o atop of which is a Gaussian profile $I_{ST}(x')=\int dk_x'|\widetilde{\psi}(k_x')|^2e^{i2k_x'x'}$ [Fig. 4(f)].

For example, for a Gaussian beam of transverse size w_o ($\frac{1}{e}$ width) and $z_R=\frac{1}{2}k_ow_o^2$ yields an on-axis ($x=0$) pulse-width $\Delta T'=\frac{k_ow_o^2}{2\gamma v}$. For $\lambda_o=2.4$ μm, $\Delta x=2w_o=40$ μm ($z_R\sim$ 0.5 mm), relative motion at $v=0.8c$ results in $\Delta T'\sim 4$ ps ($\Delta\lambda'\sim 0.25$ nm) at $\lambda_o'=800$ nm. The pulse-width is reduced to $\Delta T\sim 250$ fs when the beam width is reduced to $\Delta x=10$ μm ($\Delta\lambda'\sim 4$ nm).

Recently, STWPs were synthesized in the laboratory with $\widetilde{v}\sim c$ starting from generic pulsed beams [21]. We inquire here whether relative motion at terrestrial velocities $v\ll c$ between a quasimonochromatic source and a detector can lead to the observation of ultraslow STWPs. To investigate this possibility, we first drop the monochromaticity assumption that guarantees the formation of a detectable STWP for any v via idealized space-time coupling $\delta[\Omega'-\Omega'(k_x')]$. Rather, a realistic field is inevitably quasimonochromatic of linewidth $\delta\Omega$ in $\mathcal{O}$, corresponding to a pulse of width $\delta T\sim\frac{1}{\delta\Omega}$ traveling at a group velocity c in free space. When transformed in $\mathcal{O}'$ into an STWP, the precise delta-function correlation $\delta[\Omega'-\Omega'(k_x')]$ is relaxed to $g[\Omega'-\Omega'(k_x')]$, where $g(\cdot)$ is a narrow spectral function whose width corresponds to a *spectral uncertainty* $\delta\Omega'=\gamma(1-\beta)\delta\Omega$ [39,43].

In the paraxial regime, the field in $\mathcal{O}$ can be separated into a product of spatial and temporal envelopes

$$E(x,z;t)=e^{i(k_oz-\omega_ot)}\psi_x(x,z)\psi_t(t-z/c),\quad(4)$$

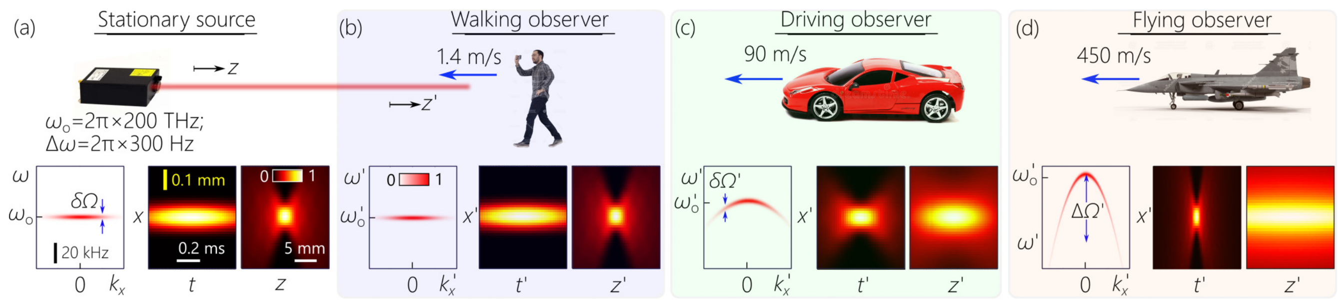

FIG. 5. Schematic of a potential test of relativistic transformations of a quasimonochromatic beam. (a) A beam from a stationary laser ($\Delta x = 100$ µm, $\frac{\omega_o}{2\pi} = 200$ THz, $\frac{\delta\Omega}{2\pi} = 300$ Hz) is recorded by moving observers. (b) A walking observer at $v = -1.4$ m/s ($\approx$5 km/h) does *not* detect any change in the beam ($|v| < v_{\min} = 40$ m/s). (c) A faster observer at $v = -90$ m/s detects a propagation-invariant STWP of pulsewidth $\Delta T' \approx 0.5$ ms traveling at a group velocity $\widetilde{v} = 90$ m/s ($\approx$320 km/h), having a spatiotemporal spectral structure $\Omega' = \Omega'(k_x')$. (d) An even faster observer at $v = -450$ m/s ($\approx$1600 km/h) observes an STWP of pulse-width $\Delta T' \approx 0.1$ ms.

where $\psi_x(x,z)$ represents the spatial diffractive dynamics at the carrier frequency ω_o and $\psi_t(t) = \int d\Omega \widetilde{\psi}(\Omega) e^{-i\Omega t}$ is a plane-wave pulse representing the temporal dynamics. The transformed field in $\mathcal{O}'$ is

$$\begin{aligned} E'(x',z';t') &= E[x', \gamma(z'+\beta ct'); \gamma(t'+\beta z'/c)] \\ &= e^{i(k_o' z' - \omega_o' t')} \psi_x[x', \gamma(z'+vt')]\psi \\ &\quad \times [\gamma(1-\beta)(t'-z'/c)]. \end{aligned} \tag{5}$$

This result corresponds to the formulation of STWPs with finite spectral uncertainty [39]. The transformed optical field separates into two terms. The first term $\psi[x', \gamma(z'+vt')]$ corresponds to an ideal propagation-invariant STWP of pulse-width $\Delta T'$ traveling at a group velocity $\widetilde{v} = -v$, whereas the second term $\psi_t[\gamma(1-\beta)(t'-z'/c)]$ represents a plane-wave pulse of width $\delta T' = \frac{\delta T}{\gamma(1-\beta)}$ traveling at c, which we term the "pilot envelope" [39]. Crucially, the Doppler-induced STWP pulse-width $\Delta T'$ is independent of the pilot envelope width $\delta T'$.

The spectral uncertainty $\delta\Omega$ in $\mathcal{O}$ sets a minimum relative velocity $v_{\min}$ between source and detector that is required for a detectable STWP

$$v_{\min} \sim 2c\left(\frac{\delta\Omega}{\omega_o}\right)\bigg/\left(\frac{\Delta k_x}{k_o}\right)^2 = k_o\frac{(\Delta x)^2}{\delta T} \sim \frac{z_R}{\delta T}, \tag{6}$$

where $\delta T \sim 1/\delta\Omega$ is the pulse-width of the field in $\mathcal{O}$.

This minimal requirement on the relative velocity can be understood from several perspectives. The spectral uncertainty $\delta\Omega$ is the finite bandwidth of the spectral support for the quasimonochromatic field on the light-cone [Fig. 2(b)]. The Doppler-induced bandwidth $\Delta\Omega'$ results in an on-axis pulse-width $\Delta T' \sim \frac{1}{\Delta\Omega'}$ that is independent of the initial linewidth. To produce a detectable STWP, the spectral tilt angle θ must produce a new spectral support on the light-cone that is distinguishable from the initial spectrum. This requires that $\Delta\Omega' > \delta\Omega'$, which sets a minimal θ, and hence a minimal relative velocity. A different perspective is gleaned from consideration of the maximum propagation distance of an STWP $L_{\max} \sim \frac{c}{\delta\Omega'|1-\cot\theta|}$ [39,43]. Observing the STWP in $\mathcal{O}'$ requires that $L_{\max}$ be larger than the axial pulse length $v\Delta T' = \frac{z_R}{\gamma}$, thereby leading to the result in Eq. (6). Indeed, the field resulting from the Lorentz transformation of a quasi-monochromatic field separates into the product of two distinct pulses of finite duration and different group velocities, which walk off after a propagation distance $L_{\max}$ corresponding to the STWP diffraction-free length [39]. For the STWP pulsewidth to be shorter than that of the pilot envelope $\Delta T' < \delta T'$ requires that $c\delta T > \frac{1-\beta}{|\beta|} z_R$.

In our simulations, we use a Gaussian pulsed beam whose spatiotemporal intensity profile in $\mathcal{O}$ is

$$I(x,z;t) \propto \frac{w_o}{w(z)} \exp\left[-\frac{2x^2}{w(z)^2} - \frac{2(t-z/c)^2}{\delta T^2}\right], \tag{7}$$

where $w(z) = w_o\sqrt{1+(z/z_R)^2}$, δT is the initial pulse-width [37], and $\frac{\omega_o}{2\pi} = 200$ THz ($\lambda_o \approx 1550$ nm). The field in $\mathcal{O}'$ is

$$\begin{aligned} I'(x',z';t') \propto &\frac{w_o}{w(\gamma[z'+vt'])} \\ &\times \exp\left[-\frac{2x'^2}{w^2(\gamma[z'+vt'])}\right. \\ &\left.-\frac{2(\gamma[1-\beta][t'-z'/c])^2}{\delta T^2}\right]. \end{aligned} \tag{8}$$

Alternatively, one may calculate the field in the spectral domain (k_x, k_z, ω) and then propagate it along z using the Fourier-transform split-step method [44,45], which yields similar results to the physical-space calculations.

We illustrate in Fig. 5 the consequences of Eq. (6) starting from a quasimonochromatic beam with $\Delta x = 100$ µm (Rayleigh range $z_R \approx 5$ mm) and spectral linewidth $\frac{\delta\Omega}{2\pi} = 300$ Hz ($\delta T = 1$ ms in $\mathcal{O}$) [Fig. 5(a)], which is observed by a moving detector [Figs. 5(b) to 5(e)]. From Eq. (6), $\beta_{\min} = 1.3\times10^{-7}$ or $v_{\min} \approx 140$ km/h, so that an observer at $v = -5$ km/h ($|v| < v_{\min}$) records a conventionally diffracting quasimonochromatic beam [Fig. 5(b)]. However, an observer at $v = -320$ km/h ($|v| > v_{\min}$) records an STWP with $\Delta T' \sim 0.5$ ms, $L_{\max} \approx 10$ mm, and $\widetilde{v} = 320$ km/h [Fig. 5(c)]. An even faster observer moving at $v = -1600$ km/h detects an STWP of shorter pulsewidth $\Delta T' \sim 100$ µs and longer propagation distance of $L_{\max} \approx 50$ mm [Fig. 5(d)].

Narrowing the linewidth to $\frac{\delta\Omega}{2\pi} = 3$ Hz reduces the threshold to $v_{\min} \approx 1.4$ km/h, and recording an STWP becomes accessible to a walking observer, whereas the flying observer records an STWP traveling freely for $L_{\max} = 5$ m. Alternatively, $v_{\min}$ can be reduced more effectively by reducing

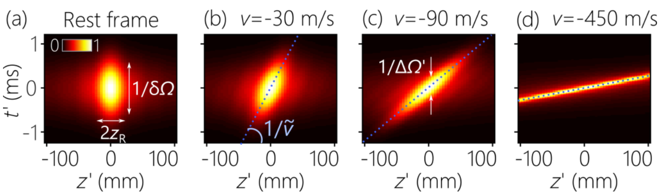

FIG. 6. On-axis intensity profile $I(x'=0,z';t')$ of a 100-μm-wide beam and 1-ms pulse duration observed in $\mathcal{O}'$ by (a) a stationary observer or observers moving towards the source at (b) $v=-30$ m/s, (c) -90 m/s, and (d) -450 m/s.

the transverse beam width due to the quadratic dependence $\beta_{\rm min}\propto(\Delta x)^2$.

We plot in Fig. 6 the on-axis intensity profiles $I(x'=0,z';t')$ with increasing v at $\frac{\delta\Omega}{2\pi}=300$ Hz, which can be viewed as world lines for the pulsed-field peak in $\mathcal{O}'$. In $\mathcal{O}$, the long temporal extent of ∼1 ms (corresponding to a length of ∼300 km) combined with the short axial extent $\Delta z=2z_{\rm R}=10$ mm renders the wave-packet *peak* effectively "stationary," even though the underlying field travels at c [Fig. 6(a)]. As the observer moves towards the source, the detected STWP can become significantly shorter than 1 ms when $v\gg v_{\rm min}$, resulting in an STWP peak moving at a group velocity $\widetilde{v}=-v$ [Figs. 6(b) to 6(d)] and propagation invariant within a 1-ms interval [Fig. 6(d)].

We consider here a model in which the laser spectrum is coherent. However, the narrow-linewidth spectra of realistic laser sources are largely *incoherent*, corresponding to continuous-wave radiation rather than pulsed [46–48]. The coherent model utilized here can be obtained by modulating the source at a rate higher than its initial linewidth to produce a train of pulses each of which is described by this model. The Lorentz transformation of a continuous-wave laser source with a spectrally incoherent linewidth requires a different analysis [49,50], which will be reported elsewhere. Furthermore, our analysis was restricted to one transverse dimension, which has the advantage of showing a clear structure (the pedestal $I_{\rm o}$) emerging as a result of space-time coupling. Incorporating both transverse dimensions does not change the conclusions except that the pedestal is replaced with a $\frac{1}{r}$ decay in intensity (r is the radial coordinate) [51–53]. In addition, the scalar field analysis can be extended to polarized fields without altering our main findings [54].

Although our strategy does not provide a more stringent test of special relativity compared to previous approaches [55–59], it may provide a simpler and more convenient testbed at terrestrial speeds in light of the current availability of ultranarrow-linewidth lasers ($\frac{\delta\Omega}{2\pi}<300$ Hz) and high-speed cameras (> 1000 frames/s). Although the Doppler shift is prohibitively difficult to detect at small β, the changes in the spatiotemporal structure of the field can be readily captured. Moreover, the results reported here may lead to new functionalities for so-called space-time metasurfaces by elucidating what can be achieved at low-speed moving devices [60–63]. Other areas in optical physics that explore the ramifications of relativistic transformations and may benefit from our results include photonic time crystals [64,65] and reflection and refraction from moving surfaces [66–71].

In summary, we analyzed a generic quasimonochromatic optical beam observed in an axially moving frame, showing that the transformed field is a propagation-invariant wave packet of finite pulse-width traveling at subluminal group velocities. Moreover, an intuitive physical picture provides the constraint on the relative velocity between the source and detector required to observe the predicted phenomena. Our analysis reveals that current technology allows for such a test to be carried out at terrestrial speeds.

Note added. Recently, a preprint appeared that reaches conclusions similar to ours [72].

The authors thank P. J. Delfyett, M. G. Vazimali, and A. Duspayev for helpful discussions. This work was funded by the U.S. Office of Naval Research (ONR), Contracts No. N00014-17-1-2458 and No. N00014-20-1-2789.

[1] A. Einstein, On the electrodynamics of moving bodies, Ann. Phys. (Leipzig) **322**, 891 (1905).
[2] D. Bohm, *The Special Theory of Relativity* (Routledge, Abingdon-on-Thames, England, 2015).
[3] E. F. Taylor and A. A. Wheeler, *Spacetime Physics: Introduction to Special Relativity*, 2nd ed. (W.H. Freeman, New York, 1992).
[4] J. D. Jackson, *Classical Electrodynamics* (John Wiley & Sons, New York, 1999).
[5] J. Terrell, Invisibility of the Lorentz Contraction, Phys. Rev. **116**, 1041 (1959).
[6] R. Penrose, The apparent shape of a relativistically moving sphere, Proc. Cambridge Philos. Soc. **55**, 137 (1959).
[7] V. F. Weisskopf, The visual appearance of rapidly moving objects, Phys. Today **13**, 24 (1960).
[8] K. Y. Bliokh and F. Nori, Relativistic Hall Effect, Phys. Rev. Lett. **108**, 120403 (2012).
[9] K. Y. Bliokh, Y. V. Izdebskaya, and F. Nori, Transverse relativistic effects in paraxial wave interference, J. Opt. **15**, 044003 (2013).
[10] K. Y. Bliokh and F. Nori, Spatiotemporal vortex beams and angular momentum, Phys. Rev. A **86**, 033824 (2012).
[11] K. Y. Bliokh, Spatiotemporal Vortex Pulses: Angular Momenta and Spin-Orbit Interaction, Phys. Rev. Lett. **126**, 243601 (2021).
[12] D. A. Smirnova, V. M. Travin, K. Y. Bliokh, and F. Nori, Relativistic spin-orbit interactions of photons and electrons, Phys. Rev. A **97**, 043840 (2018).
[13] S. Akturk, X. Gu, P. Gabolde, and R. Trebino, The general theory of first-order spatio-temporal distortions of Gaussian pulses and beams, Opt. Express **13**, 8642 (2005).
[14] S. Akturk, X. Gu, P. Bowlan, and R. Trebino, Spatio-temporal couplings in ultrashort laser pulses, J. Opt. **12**, 093001 (2010).
[15] P. A. Bélanger, Lorentz transformation of packetlike solutions of the homogeneous-wave equation, J. Opt. Soc. Am. A **3**, 541 (1986).
[16] P. Saari and K. Reivelt, Generation and classification of localized waves by Lorentz transformations in Fourier space, Phys. Rev. E **69**, 036612 (2004).

[17] J. N. Brittingham, Focus wave modes in homogeneous Maxwell's equations: Transverse electric mode, J. Appl. Phys. **54**, 1179 (1983).
[18] P. Saari and K. Reivelt, Evidence of X-Shaped Propagation-Invariant Localized Light Waves, Phys. Rev. Lett. **79**, 4135 (1997).
[19] J. Turunen and A. T. Friberg, Propagation-invariant optical fields, Prog. Opt. **54**, 1 (2010).
[20] *Non-Diffracting Waves*, edited by H. E. Hernández-Figueroa, E. Recami, and M. Zamboni-Rached (Wiley-VCH, Weinheim, 2014).
[21] M. Yessenov, A. A. Hall, K. L. Schepler, and A. F. Abouraddy, Space-time wave packets, Adv. Opt. Photon. **14**, 455 (2022).
[22] F. Wilczek, *A Beautiful Question: Finding Nature's Deep Design* (Penguin, New York, 2015).
[23] L. Mackinnon, A nondispersive de Broglie wave packet, Found. Phys. **8**, 157 (1978).
[24] H. E. Kondakci and A. F. Abouraddy, Diffraction-free pulsed optical beams via space-time correlations, Opt. Express **24**, 28659 (2016).
[25] K. J. Parker and M. A. Alonso, The longitudinal iso-phase condition and needle pulses, Opt. Express **24**, 28669 (2016).
[26] L. J. Wong and I. Kaminer, Ultrashort tilted-pulsefront pulses and nonparaxial tilted-phase-front beams, ACS Photon. **4**, 2257 (2017).
[27] N. K. Efremidis, Spatiotemporal diffraction-free pulsed beams in free-space of the Airy and Bessel type, Opt. Lett. **42**, 5038 (2017).
[28] M. A. Porras, Gaussian beams diffracting in time, Opt. Lett. **42**, 4679 (2017).
[29] M. Yessenov, B. Bhaduri, H. E. Kondakci, and A. F. Abouraddy, Classification of propagation-invariant space-time light-sheets in free space: Theory and experiments, Phys. Rev. A **99**, 023856 (2019).
[30] H. E. Kondakci and A. F. Abouraddy, Optical space-time wave packets of arbitrary group velocity in free space, Nat. Commun. **10**, 929 (2019).
[31] H. E. Kondakci and A. F. Abouraddy, Self-healing of space-time light sheets, Opt. Lett. **43**, 3830 (2018).
[32] B. Bhaduri, M. Yessenov, and A. F. Abouraddy, Anomalous refraction of optical space-time wave packets, Nat. Photon. **14**, 416 (2020).
[33] S. Longhi, Gaussian pulsed beams with arbitrary speed, Opt. Express **12**, 935 (2004).
[34] H. E. Kondakci and A. F. Abouraddy, Airy Wave Packets Accelerating in Space-Time, Phys. Rev. Lett. **120**, 163901 (2018).
[35] R. Donnelly and R. W. Ziolkowski, Designing localized waves, Proc. R. Soc. London A **440**, 541 (1993).
[36] J. W. Goodman, *Fourier Optics* (Roberts & Company, Greenwood Village, CO, 2005).
[37] B. E. A. Saleh and M. C. Teich, *Principles of Photon.* (Wiley, New York, 2007).
[38] H. E. Kondakci and A. F. Abouraddy, Diffraction-free space-time beams, Nat. Photon. **11**, 733 (2017).
[39] M. Yessenov, B. Bhaduri, L. Mach, D. Mardani, H. E. Kondakci, M. A. Alonso, G. A. Atia, and A. F. Abouraddy, What is the maximum differential group delay achievable by a space-time wave packet in free space? Opt. Express **27**, 12443 (2019).
[40] M. Moshinsky, Diffraction in time, Phys. Rev. **88**, 625 (1952).
[41] M. Moshinsky, Diffraction in time and the time-energy uncertainty relation, Am. J. Phys. **44**, 1037 (1976).
[42] S. Godoy, Diffraction in time: Fraunhofer and Fresnel dispersion by a slit, Phys. Rev. A **65**, 042111 (2002).
[43] H. E. Kondakci, M. A. Alonso, and A. F. Abouraddy, Classical entanglement underpins the propagation invariance of space-time wave packets, Opt. Lett. **44**, 2645 (2019).
[44] M. S. Wartak, *Computational Photon.: An Introduction with MATLAB* (Cambridge University Press, Cambridge, England, 2013).
[45] M. Yessenov and A. F. Abouraddy, Accelerating and Decelerating Space-Time Optical Wave Packets in Free Space, Phys. Rev. Lett. **125**, 233901 (2020).
[46] C. H. Henry, Theory of the linewidth of semiconductor lasers, IEEE J. Quantum Electron. **18**, 259 (1982).
[47] C. H. Henry and R. F. Kazarinov, Quantum noise in photonics, Rev. Mod. Phys. **68**, 801 (1996).
[48] M. Pollnau and M. Eichhorn, Spectral coherence, Part I: Passive-resonator linewidth, fundamental laser linewidth, and Schawlow-Townes approximation, Prog. Quantum Electron. **72**, 100255 (2020).
[49] M. Yessenov, B. Bhaduri, H. E. Kondakci, M. Meem, R. Menon, and A. F. Abouraddy, Non-diffracting broadband incoherent spacetime fields, Optica **6**, 598 (2019).
[50] M. Yessenov and A. F. Abouraddy, Changing the speed of coherence in free space, Opt. Lett. **44**, 5125 (2019).
[51] C. Guo, M. Xiao, M. Orenstein, and S. Fan, Structured 3D linear spacetime light bullets by nonlocal nanophotonics, Light: Sci. Appl. **10**, 160 (2021).
[52] M. Yessenov, J. Free, Z. Chen, E. G. Johnson, M. P. J. Lavery, M. A. Alonso, and A. F. Abouraddy, Space-time wave packets localized in all dimensions, Nat. Commun. **13**, 4573 (2022).
[53] K. Pang, K. Zou, H. Song, M. Karpov, M. Yessenov, Z. Zhao, A. Minoofar, R. Zhang, H. Song, H. Zhou, X. Su, N. Hu, T. J. Kippenberg, A. F. Abouraddy, M. Tur, and A. E. Willner, Synthesis of near-diffraction-free orbital-angular-momentum space-time wave packets having a controllable group velocity using frequency comb, Opt. Express **30**, 16712 (2022).
[54] W. Cocke and D. Holm, Lorentz transformation properties of the Stokes parameters, Nat. Phys. Sci. **240**, 161 (1972).
[55] H. E. Ives and G. R. Stilwell, An experimental study of the rate of a moving atomic clock, J. Opt. Soc. Am. **28**, 215 (1938).
[56] J. C. Hafele and R. E. Keating, Around-the-world atomic clocks: Observed relativistic time gains, Science **177**, 168 (1972).
[57] R. Mansouri and R. U. Sexl, A test theory of special relativity: III. Second-order tests, Gen. Relativ. Gravit. **8**, 809 (1977).
[58] P. Wolf, S. Bize, M. E. Tobar, F. Chapelet, A. Clairon, A. N. Luiten, and G. Santarelli, Recent experimental tests of special relativity, in *Special Relativity*, edited by J. Ehlers and C. Lämmerzahl (Springer, New York, 2006), pp. 451–478.
[59] C. W. Chou, D. B. Hume, T. Rosenband, and D. J. Wineland, Optical clocks and relativity, Science **329**, 1630 (2010).
[60] Z. L. Deck-Léger, N. Chamanara, M. Skorobogatiy, M. G. Silveirinha, and C. Caloz, Uniform-velocity spacetime crystals, Adv. Photon. **1**, 056002 (2019).
[61] C. Caloz and Z.-L. Deck-Léger, Spacetime metamaterials–Part I: General, IEEE Trans. Antennas Propag. **68**, 1569 (2020).

[62] C. Caloz and Z.-L. Deck-Léger, Spacetime metamaterials–Part II: Theory and applications, IEEE Trans. Antennas Propag. **68**, 1583 (2020).

[63] P. Rocca, A. Alú, C. Caloz, and S. Yang, Guest editorial: Special cluster on space-time modulated antennas and materials, Antennas Wirel. Propag. Lett. **19**, 1838 (2020).

[64] M. Lyubarov, Y. Lumer, A. Dikopoltsev, E. Lustig, Y. Sharabi, and M. Segev, Amplified emission and lasing in photonic time crystals, Science **377**, 425 (2022).

[65] Y. Sharabi, A. Dikopoltsev, E. Lustig, Y. Lumer, and M. Segev, Spatiotemporal photonic crystals, Optica **9**, 585 (2022).

[66] B. W. Plansinis, W. R. Donaldson, and G. P. Agrawal, What is the Temporal Analog of Reflection and Refraction of Optical Beams?, Phys. Rev. Lett. **115**, 183901 (2015).

[67] H. Qu, Z.-L. Deck-Léger, C. Caloz, and M. Skorobogatiy, Frequency generation in moving photonic crystals, J. Opt. Soc. Am. B **33**, 1616 (2016).

[68] B. W. Plansinis, W. R. Donaldson, and G. P. Agrawal, Temporal waveguides for optical pulses, J. Opt. Soc. Am. B **33**, 1112 (2016).

[69] B. W. Plansinis, W. R. Donaldson, and G. P. Agrawal, Single-pulse interference caused by temporal reflection at moving refractive-index boundaries, J. Opt. Soc. Am. B **34**, 2274 (2017).

[70] B. W. Plansinis, W. R. Donaldson, and G. P. Agrawal, Cross-phase-modulation-induced temporal reflection and waveguiding of optical pulses, J. Opt. Soc. Am. B **35**, 436 (2018).

[71] Z.-L. Deck-Léger, X. Zheng, and C. Caloz, Electromagnetic wave scattering from a moving medium with stationary interface across the interluminal regime, Photonics **8**, 202 (2021).

[72] D. Ramsey, A. Di Piazza, M. Formanek, P. Franke, D. H. Froula, B. Malaca, W. B. Mori, J. R. Pierce, T. T. Simpson, J. Vieira, M. Vranic, K. Weichman, and J. P. Palastro, Exact solutions for the electromagnetic fields of a flying focus, Phys. Rev. A **107**, 013513 (2023).